

Conservative numerical methods for model kinetic equations

V. A. Titarev

Laboratory of Applied Mathematics
Department of Civil and Environmental Engineering
University of Trento, Trento, Italy
[E-mail: titarev@ing.unitn.it](mailto:titarev@ing.unitn.it), titarev@mail.ru

Abstract

A new conservative discrete ordinate method for nonlinear model kinetic equations is proposed. The conservation property with respect to the collision integral is achieved by satisfying at the discrete level approximation conditions used in deriving the model collision integrals. Additionally to the conservation property, the method ensures the correct approximation of the heat fluxes. Numerical examples of a supersonic flow with large gradients are provided for the Shakhov and Rykov model kinetic equations.

Key words: rarefied, low Knudsen numbers, kinetic equation, Shakhov model, Rykov model, conservative method.

1 Introduction

Correct description of rareed gas ows is based on the Boltzmann kinetic equation for the molecular velocity distribution function. Since this integro-dierential equation is exceedingly complicated due to the presence of the nonlinear multidimensional collision integral much attention has been given to simpler model kinetic equations. These equations are constructed by replacing the exact collision integral by an approximate model collision integral. Examples include the Krook or BGK [6], Holway [12] and Shakhov [26, 28] model equations for monatomic gases as well as Holway [12] and Rykov [24] model equations for diatomic gases.

Numerical solution of kinetic equations requires the use of conservative methods suitable in a broad range of Knudsen numbers (including transitional and low Knudsen numbers) and for both steady and unsteady ow regimes. In recent years considerable progress has been made in devising such methods for the kinetic equation with the exact Boltzmann collision integral [7, 23, 5]. For model equations the situation is less clear. Conservative discrete ordinate methods proposed for simple monatomic BGK and Holway model equations [22, 11] cannot be extended directly to the Shakhov and Rykov models. A rather sophisticated correction procedure was applied in [10] to the Shakhov model collision integral at each time step in such a way as to satisfy the conservation property. Its generalization to other models has not been reported. No conservative method has so far been developed for diatomic models.

The purpose of this paper is to present an exceedingly simple and universal approach to construction of conservative discrete ordinate methods for model kinetic equations. The approach is an extension of [33] and is based on the approximation of the constrains used in deriving the model equations. Therefore, it can be used for virtually any model kinetic equation. We provide a detailed explanation of the idea as applied to the Shakhov model equation and then extend it to the Rykov model equation.

As a numerical example, we consider a supersonic transverse ow over a flat plate for a wide range of Knudsen numbers from free-molecular to near-continuum regime using both model equations. The presented results illustrate the sensitivity of the method to the choice of the molecular velocity mesh as well as provide a study of aerodynamic properties of the plate and distribution of the macroscopic parameters.

2 Monatomic gases

2.1 Construction of model equations

For monatomic gases a general approach to construction of model kinetic equations was proposed in [25, 28] and is based on the idea of approximating the exact Boltzmann kinetic equation in terms of momentum equations. In other words few rst momentum equations should coincide for the model and exact kinetic equations. As a result, a sequence of model kinetic equations can be developed by increasing the order of moments for which

the approximation condition holds.

Let us write the model kinetic equation for the velocity distribution function f in the following form:

$$\frac{df}{dt} + \frac{df}{dr} = Q(f, a) \quad (1)$$

Here $r = (x_1, x_2, x_3)$ is the molecular velocity vector, t is time, $r = (x_1, x_2, x_3)$ is the spatial coordinate, a is an unknown vector of macroscopic parameters which depends on the chosen model equation. Since the differential parts of the exact and model equations are the same, the approximation condition means that the first few moments of the exact collision integral $J(f)$ coincide with the first few moments of the model collision integral $Q(f, a)$:

$$\int Q(f, a) d^3v = \int J(f) d^3v = J \quad (2)$$

where

$$J = \int v_i^2 v_j v_i v_j v_k d^3v$$

Alternatively one can use

$$\int v_i v_j v_k d^3v = U$$

As is common in construction of model kinetic equations for the monatomic gas it is assumed that the approximation condition (2) should be satisfied for the Maxwellian molecules only. Then the moments J can be evaluated analytically and we can express the vector a via the integrals of the velocity distribution function:

$$U(a) = b(v) f d^3v \quad (3)$$

where U is a certain function of macroscopic parameters and $b(v)$ is a vector function of the molecular velocity.

2.2 The model of Shakhov

The Shakhov model kinetic equation is a generalization of the Krook model equation in that the approximation condition (2) is satisfied not only for $\int v_i^2 v_j v_i v_j v_k d^3v$, but also for $\int v_i^2 v_j v_i v_j v_k d^3v$. This ensures the correct relaxation of both the heat flux and stresses, leading thus to the correct continuum limit in the case of small Knudsen numbers. In particular, the model gives the correct Prandtl number. Comparisons of different monatomic model equations with experimental data and the numerical solution of the Boltzmann equation with the exact collision integral shows the Shakhov model to be more accurate than the BGK and Holway models [38, 30].

In the rest of the paper we use the non-dimensional form of the kinetic equations in which non-dimensional spatial variable r , time t , number density n , velocities u and ,

temperature T , viscosity μ , heat flux q and distribution function f are given by

$$\begin{aligned} r' &= \frac{r}{L}, & t' &= \frac{t\sqrt{2RT_\infty}}{L}, & n &= \frac{n}{n_\infty}, & u &= \frac{u}{\sqrt{2RT_\infty}} \\ T' &= \frac{T}{T_\infty}, & \mu' &= \frac{\mu}{\mu_\infty}, & q &= \frac{q}{\mu_\infty}, & f &= \frac{f}{f_\infty} \end{aligned} \quad (4)$$

Here L is a typical spatial scale of the problem, n_∞ , R is the gas constant, T_∞ - some characteristic values of gas density and temperature; m is the molecule mass, λ is the mean free path connected to μ by

$$\lambda = \frac{5}{16mn\sqrt{2RT}}$$

Below we shall use the conventional notation for all variables meaning the non-dimensional quantities.

In the non-dimensional form the Shakhov model collision integral is given by [26, 28]

$$Q(f, a) = f_+ - f \quad \text{with } \frac{8}{5} \frac{nT}{\mu} = \text{Kn} \quad \text{and } \frac{2}{5} \frac{q}{\mu} = \text{Pr}$$

$$f_+ = f_M \left[1 + \frac{4}{5} \frac{\text{Pr}^{2qv}}{nT} \left(\frac{v_2}{T} \right)^2 \right] \exp\left(-\frac{v^2}{2T}\right)$$

Here f_M is the locally-maxwellian function, $\text{Kn} = L/\lambda$ and Pr are the Knudsen and Prandtl numbers, respectively. The vector of unknown parameters in the model collision integral $a = (nuTq)^T$ containing number density n , temperature T and vectors of gas velocity u and heat flux q can be calculated as:

$$U(a) = \int n \nu u^3 + 2nT + nu^2 2q(1^2 v v^2) f d =$$

Since the expression for f_+ contains the third-order polynomial of the distribution function f may become negative at the tails. Although a possible loss of positivity is a drawback from the theoretical point of view, it does not affect the robustness of the model in practical applications because $f \geq 0$ almost everywhere. For example, see [3] for the numerical study of the structure of exceedingly strong shock waves (Mach numbers up to 100) and [34] for calculation of the hypersonic *transverse* flow over a cold plate with free-stream Mach numbers up to $M=30$. Moreover, according to the Godunov theorem [9], second-order advection schemes with linear operators often used in practice [1, 34] are not monotone and may generate the negative values of f even for the BGK model, further diminishing the importance of strict theoretical positivity.

The H theorem for the Shakhov model can be proven only for flows with small departures from equilibrium [28]. We remark, however, that the problem of spatially-homogenous relaxation to equilibrium admits an exact solution for the Shakhov model equation with the correct relaxation of all non-equilibrium moments of the distribution function as well as the H function, see e.g. [28]. This fact constitutes an indirect evidence that the H theorem holds for the Shakhov model equation.

2.3 Conventional discrete ordinate method

A standard approach to solve the model kinetic equation with given boundary and initial conditions is the so-called discrete ordinate method. Its main idea is to replace the exact integration with respect to molecular velocity over all velocity space by an approximate numerical integration over a finite domain using a discrete set of points. Let i be an index of the three-dimensional molecular velocity mesh, r_i be a node in this mesh, $f = f(t, r)$. Then the model kinetic equation is replaced by a system of equations for f_i :

$$\frac{df_i}{dt} = Q_i - Q_i = Q_i(f, a) \quad (7)$$

which are connected via macroscopic parameters defined as integrals over the entire molecular velocity space. Each of equations (7) can now be solved using a modern high order non-oscillatory scheme. For example, an *explicit* semi-discrete scheme can be written as

$$f_i = D_h(f) + Q_i \Delta t$$

where D_h is a conservative numerical approximation to the advection operator. A review of modern approaches to the construction of such operators can be found in many references, e.g. [35, 17, 31]. For example, in the spatially one-dimensional case the expression for D_h reduces to

$$(D_h(f))_i = \frac{f_{i+1/2} - f_{i-1/2}}{\Delta x_i}$$

where i is the index of the spatial mesh, Δx_i is the cells size. The values of the distribution function at the cell interfaces $f_{i+1/2}$ can be computed using a second-order MUSCL-type reconstruction [15, 16, 36] or higher order reconstruction, e.g. finite-difference or finite-volume weighted essentially non-oscillatory reconstructions [14, 31].

Conventionally, e.g. [37], macroscopic parameters are evaluated by direct approximation of (3).

$$U(a) = \int f a \quad (9)$$

For the Shakhov model this gives:

$$\begin{aligned} \frac{1}{3} \int v v^2 f A(10) \\ n u = \frac{2}{3} n T + n u^2 2q \end{aligned}$$

Here A are weights of the integration rule used in the numerical scheme. Normally one uses a tensor product of one-dimensional quadrature to perform the three-dimensional integration in the molecular velocity space, e.g. the simplest choice corresponds to the first order quadrature and is given by $A = \frac{1}{3}$.

2.4 Conservation property

It is well known that the conservation laws for mass, momentum and energy of the gas can be obtained by multiplying (1) by collision invariants $1, v, v^2$ and integrating over the

entire molecular velocity space. It is natural to require that this property be maintained at the discrete level by the numerical method (8),(9). The discrete relations expressing conservation of mass, momentum and energy in the computations are obtained by multiplying (8) by the collision invariants and summing them with the weights A :

$$R + D_h(\cdot) = \kappa_n$$

Here the vector of conserved quantities R , the ux tensor ij and the numerical source term $(a Kn)\kappa_n$ on the right hand side are given by

$$R = I f \quad A = I_T f \quad A_{\kappa_n} = I Q A \quad I = (1^2)^T$$

It is obvious, that R coincides with rst ve components of U dened by (10).

Following [4] we call the numerical method (8) conservative with the respect to the collision integral if the numerical source term vanishes: $\kappa_n = 0$. Basically, conservative methods mimic the conservation property of the collision integral on a given molecular velocity grid. They do not produce non-physical sources of mass, momentum and energy and therefore in the limit of small Knudsen numbers the kinetic solution approaches the solution of Navier-Stokes equations away from boundaries. On the contrary, as will be shown below, for non-conservative methods very ne meshes in the molecular velocity space are needed to keep the conservation error small when the Knudsen number decreases.

We now demonstrate that for any choice of the quadrature weights A and cell size the conventional discrete ordinate method, given by (8), (10) is not conservative. Using (10) we can rewrite the expression for the source term κ_n in the following form:

$$\kappa_n = \begin{pmatrix} \sum_{\beta} f_{\beta}^+ A_{\beta} - n \\ \sum_{\beta} \xi_{\beta} f_{\beta}^+ A_{\beta} - n \\ \sum_{\beta} \xi_{\beta}^2 f_{\beta}^+ A_{\beta} - n \end{pmatrix} \begin{matrix} \\ 2T + u^2 \\ \end{matrix} \quad (12)$$

The exact integration of f^+ with respect to gives

$$(1^2) f^+ d = n \quad n u \quad n \quad 2T + u^2$$

However, the r th order quadrature with weighs A used in the discrete ordinate method yields

$$(0) \quad (1^2) f^+ A = n \quad n u \quad n \quad 2T + u^2 + O(r)$$

Substituting the above expressions into (12) we can estimate the norm of the numerical

$$\text{source term as} \quad \kappa_n = O(r) \quad 1 \text{ Kn} O(r) \quad (14)$$

From (14) it is obvious that for a given molecular velocity mesh the conventional discrete ordinate method applied to the nonlinear Shakhov model equation produces a source term that grows $\propto n$ as $Kn \rightarrow 0$. Moreover, the same behaviour can be observed for the linearized kinetic equations (details are omitted). In the case of small Knudsen numbers κ_n can be very large. In practical calculations one cannot afford a

fine mesh for due to excessive memory requirements. As a result, computations with small Knudsen number may become difficult. For example, it follows from the above argument that the free-stream conditions cannot be preserved exactly.

In addition to the conservation property, one would also like the numerical integration with respect to \mathbf{v} to reproduce the exact values of macroscopic parameters when f is given in the form of the locally Maxwellian function. This is called *compatibility with the initial distribution of macroscopic parameters* [4]. The conventional discrete-ordinate method is not compatible with the initial data because the macroscopic parameters are computed with an error of order of $(\Delta v)^2$, see (13). Due to the presence of the large numerical source term κ_n , this error may grow rapidly with time.

A similar conservation error occurs at the boundary; however, it does not depend directly on the Knudsen number and in many cases can be simply ignored.

2.5 Construction of the explicit conservative method

The explicit conservative method is obtained by modifying the discrete collision integral

$$\frac{df}{dt} = D_r(f) + Q(f, a) \quad (15)$$

where the modified vector of macroscopic parameters a is obtained as a solution of the discrete approximation to (2)

$$Q(f, a)A = J \quad (16)$$

For the Shakhov model equation it is convenient to use $\mathbf{v} = \frac{1}{2} v^2$. Then first five equations in (16) represent conservation of mass, momentum and energy of colliding molecules; the corresponding moments J vanish. The conservation conditions (16) can be written as:

$$QA = \begin{pmatrix} 1 & 0 \\ & 0 \\ & 0 \\ & 0 \\ & 0 \end{pmatrix} \begin{pmatrix} 0 \\ 0 \\ 0 \\ 0 \\ 0 \end{pmatrix} \quad (17)$$

The nonlinear system (17) for (n, u, T, q) can be easily solved by the Newton iteration method. The iteration process requires an initial guess which is provided by the conventional expressions (9), (10). Usually, it is sufficient to make one or two iterations since the Newton process converges very rapidly.

It is obvious that the modified method (15), (16) is conservative by construction for any choice of the quadrature weights A , including the first order quadrature, and any value of the Knudsen number Kn . However, since

$$a = a + O(\Delta t)$$

the use of higher-order quadratures results in a better initial guess (10) and thus faster convergence of iterations. Naturally, smaller values of Kn require more iterations. The choice of the cell size of the molecular velocity mesh also plays a role: the smaller is the faster iterations converge; normally we use 72 . See the section of numerical

results for a numerical study of the influence of Δt on the accuracy of the results.

The conservation property holds for the macroscopic parameters a defined by the conventional expression (10). Although on a sufficiently fine molecular velocity mesh a and q differ only slightly, on a coarse mesh a is a more accurate approximation to the macroscopic parameters. Therefore, while presenting results of computations, we always use the modified vector a rather than a . Since the model collision integral Q is an infinitely smooth function of all variables the formal approximation order of the modified discrete ordinate method (15) is equal to that of the conventional one.

The BGK model collision integral does not contain the values of q and thus it is sufficient to use only the first five equations in (17), see [22, 11].

2.6 Implicit methods

We have considered explicit advection schemes only. For steady-state applications, however, one-step implicit schemes are more frequently used. On the construction of such schemes see e.g. [37, 22]. The essential difference of the implicit scheme from the explicit method (15) is the presence of an additional differential operator in front of the temporal derivative. This operator is approximated by first-order upwind differences and makes the scheme unconditionally stable; it also leads to the appearance of an additional numerical source term and thus to the loss of the global conservation property. However, it vanishes in the steady-state and we again have the correct approximation to the conservation laws. We also note that for time-dependent calculations the source term is small due to the condition $\Delta t < 1$ and therefore can be neglected. The details are omitted.

3 Extension to diatomic gases

3.1 The model of Rykov

For the diatomic gas the distribution function now depends not only on t, r, v , but also on the energy of rotational movement e . The Rykov model kinetic equation has the form (1) with the collision integral given by [24]:

$$Q(f, a) = \int f(r + \Delta r, v + \Delta v) f(t + \Delta t) f(18)$$

Here ν_r, ν_t are the frequencies of nonelastic and elastic collisions, f_r, f_t are the distribution functions of molecules after nonelastic and elastic collisions, respectively. Let us introduce the following reduced distribution functions [24]

$$f_0(t, r) = f_0^d e f_1(t, r) = e f_0^d e$$

Multiplying (18) by 1, e and integrating with respect to e we obtain the following non-dimensional system for f_0, f_1 :

$$\frac{f_k}{t} + \frac{f_k}{r} = H_k H_k(f_k a) = r f_{rk} + t f_{tk} (\nu_r + \nu_t) f_{kk} = 0 \quad (19)$$

where

$$r = \frac{8}{8 q_t} \frac{1}{5} \frac{n T_t}{K n} \frac{1}{v^2} \frac{1}{5} \quad K = n \quad Z = \frac{8}{8} \frac{1}{q_t} \frac{n T_t}{v^2} \frac{1}{5} \quad Z_t =$$

$$f_{r0} = f_M(T) \frac{1}{15} + f_{t0} = f_M(T) \frac{1}{15} + \frac{q_r v}{15 p T} \frac{1}{T^2}$$

$$f_{r1} = T f_{r0} + 4 \frac{1}{52 T} \left(\frac{q_r v}{p T} \right) T f_M(T) \frac{q_r v}{p T} \quad f_{t1} = T f_{t0} + 4 \frac{1}{n T_t p} \left(\frac{q_r v}{p T} \right) \frac{q_r v}{p T}$$

$$52 T \frac{3}{2} \frac{T_r + T_p}{T} = n T_t p = n T = 1155$$

Here $\nu_t = (\nu_r + \nu_t)$ -viscosity, T_t, T_r translational and rotational temperatures, T average temperature, q_t, q_r translational and rotational heat fluxes, $Z = Z(T_r, T_t)$ is ratio of the number of collisions to the number of rotational (nonelastic) collision. Expressions for ν_t and $Z(T_r, T_t)$ can be found in [24, 18, 19]:

$$\nu_t = T_{23} \frac{(B)}{t(B, T_t)} \frac{T}{B = T} \quad T_r W = T_t$$

$$\frac{3.9 B T_t W}{Z(T_t, T_r)} = 0.461 + 0.5581 W + \frac{0.0358 W^{2(BT_t)}}{8} \quad (B, T_t)^{16}$$

The expression for Z approximates the results of [21]. For nitrogen we have [20]

$$T = 915^\circ K_0 = 0.2354 T_1 = 0.3049$$

These values of $\nu_{0,1}$ are found from the conditions that the heat conductivity coefficient obtained from the model kinetic equations is equal to its experimentally found value.

3.2 Approximation conditions and macroscopic parameters

For the Rykov model the vector a in the model collision integral is given by

$$a = (n u \quad T_t T_r q^t \quad q^r)^T$$

The approximation conditions (2) on the model collision integral which are used to determine the expressions for the vector a in terms of the distribution function can be written as follows:

$$\begin{pmatrix} H_0 \\ H_0 \\ 2H_0 + H_1 \\ H_1 \\ vV_2 H_0 \\ vH_1 \end{pmatrix} d = \begin{pmatrix} 0 \\ 0 \\ 0 \\ (32)n (T_t T) \\ (43 + 2(1_0) 3 Z) Z \cdot q^t \\ (2 + 2(1_1)(1)Z) Z \cdot q^r \end{pmatrix} \quad (20)$$

The first six equations represent conservation laws of mass, momentum and energy and include the relaxation of translational and rotational temperatures to the average gas temperature. The last six equations represent the conditions for relaxation of translational and rotational heat fluxes.

Performing exact integration in (20) we obtain the following expressions for macroscopic parameters:

$$\begin{aligned} \frac{3}{2} n T_t + n u_2 &= (1^2) f_0 d n n u = \\ q_t &= v v \int f d n T_r = f d q^r = 1 v f d \\ 2 & \quad 2 \end{aligned}$$

Note that when the rotational degrees of freedom are frozen ($Z = 0$), the Rykov model reduces to the Shakhov model.

3.3 The conservative discrete ordinate method

The conservative version of the discrete ordinate method for the Rykov model is a direct extension of the monatomic version from the previous section. The basic idea is again to modify the vector of macroscopic parameters in used in the model collision integral so that to ensure the conservation property.

Let us denote the values of f_k in the velocity nodes by $f_k = f_k(t, r)$. The conservative discrete ordinate method (8) is now written as:

$\underline{f}_k = D_n (f_k) + H_k (f_k a)$ $k = 0, 1, t$
 where the modified vector of macroscopic parameters a is obtained by solving the following system of equations:

$$\begin{pmatrix} H_0 \\ H_0 \\ 2H_0 + H_1 \\ H_1 \\ vV_2 H_0 \\ vH_1 \end{pmatrix} A = \begin{pmatrix} 0 \\ 0 \\ 0 \\ (32)n (T_t T) \\ (43 + 2(1_0) 3 Z) Z \cdot q^t \\ (2 + 2(1_1)(1)Z) Z \cdot q^r \end{pmatrix} \quad (23)$$

The system (23) is a direct approximation of (20) on the given molecular velocity mesh and is solved by the Newton iteration method. The first guess is provided by the conventional expressions of the form:

$$3 \quad n n u_2 n T_t + n u^2 (1^2) f_0 A =$$

$$q_t = \frac{1}{2} \quad v v_2 \quad f_0 A \quad n T_r = \quad f_1 A \quad q_r = \frac{1}{2} \quad v f_1 A$$

As for the monatomic model, the method given by (23) remains conservative for any Kn and A. The choice of the quadrature is motivated by the same arguments as for the Shakhov model.

4 Numerical examples

To illustrate the advantages and robustness of the proposed conservative procedure for evaluating macroscopic parameters we calculate two flows: cylindrical Couette flow and supersonic transverse flow over a flat plate.

4.1 Cylindrical Couette flow

4.1.1 Statement of the problem

A detailed setup of the conventional problem can be found in many papers, e.g. [32, 29, 2]. Consider a steady-state flow between two infinite coaxial cylinders with radii $r_1 < r_2$. The outer cylinder is at rest. The gas flows due to the rotation of the inner cylinder with a constant angular velocity Ω . On the surfaces of the cylinders a constant temperature T_w (the same for both cylinders) is maintained.

We introduce the cylindrical coordinate system (r, θ, z) , where the z axis coincides with the axis of the cylinders, r is the distance from this axis, and θ is the azimuthal coordinate. In velocity space we also introduce a cylindrical coordinate system with the z axis parallel to the z axis. We will denote by v_r the velocity component in a plane perpendicular to the axis of the cylinders and by α the angle between this component and the radial direction outward from the symmetry axis so that $v_r = v \cos \alpha$, $v_\theta = v \sin \alpha$.

We use the non-dimensional variables, in which the scales of the spatial coordinate r , temperature T , and density are given by

$$\frac{r}{r_2} = \frac{r - r_1}{r_2 - r_1}, \quad \frac{T}{T_w} = \frac{T - T_w}{T_0 - T_w}, \quad n = \frac{n_0}{n_0} \quad (0)$$

$$n_0 = \frac{2}{r_2 - r_1} \int_{r_1}^{r_2} n(r) dr$$

Here, n_0 is the problem can be mean density of the gas between the cylinders. reduced by integrating with respect to z [8] and

The dimension of the passing from f to the

vector of reduced distribution function g :

$$g = \int_0^{2\pi} \int_0^{\pi} f_z d\Omega$$

In non-dimensional variables the kinetic equation for g in the cylindrical coordinate system can be written in the following conservative form:

$$\frac{\partial}{\partial t} (G \cdot g) + \text{div}(g \sin) + rHH = (G g) \quad (26)$$

where the components of G and the collision frequency are given by

$$G = g_M \frac{1 + 5(1 - \text{Pr})(S_r c_r + S_c)(c_{2r} + c_2)}{4} \\ (12) T \frac{1 + 5(1 - \text{Pr})(S_r c_r + S_c)(c_{2r} + c_2)}{4} \\ g_M = \frac{n}{T} \exp(-c^2) = \frac{8}{5} \frac{n T}{Kn}$$

Here, $Kn = \lambda_0 / r$ is the Knudsen number, which determines the degree of gas rarefaction; λ_0 is the free path in the gas at rest with density n_0 and temperature T_w . The gas density n , velocity u , temperature T and heat fluxes q_s , q can be expressed in terms of the distribution function g in the form of integrals with respect to the molecular velocity

$$\begin{aligned} n &= \int_0^{2\pi} \int_0^{\pi} g d\Omega \\ n u &= \int_0^{2\pi} \int_0^{\pi} g c d\Omega \\ n T &= \int_0^{2\pi} \int_0^{\pi} g c^2 d\Omega \\ q_s &= \int_0^{2\pi} \int_0^{\pi} g c c_s d\Omega \\ q &= \int_0^{2\pi} \int_0^{\pi} g c c \cdot d\Omega \end{aligned} \quad (27)$$

The expressions for the boundary conditions on the surfaces of the cylinders are omitted.

4.1.2 Method of the solution

The steady-state solution of the problem is found by marching in time to the steady state. Let us denote $t = t_n$, $g_n = g(t_n, r)$, $r = r_n = r(t_n, g_n)$. Since we are not interested in correct approximation of the unsteady transition regime from the initial distribution function to the steady state a fully implicit difference scheme for kinetic equation (26) is used. The scheme can be written in the following form [13, 37]:

$$\frac{1}{t} + \frac{c}{r} \cos \theta \sin \theta + \dots = K^n \quad (28)$$

$$K_n = (r \cos \theta)^n + \frac{1}{2} (\sin \theta)^{n+1} H^n(r)$$

Next in variables r, θ we introduce a finite-volume mesh with cell centers r_i, θ_j that is refined toward the surfaces of the cylinders. With respect to θ we use a uniform mesh with

nodes k and cell size Δr . The derivatives in the right-hand side are approximated using a second-order non-oscillatory reconstruction technique described in [15, 16, 36]. Then, the range of r is divided into four subdomains depending on the sign of the molecular

velocity components v_r ; $v_r \in [m_1 \Delta r, m_2 \Delta r]$, where $m = 0, 1, 2, 3$. For each subdomain, the derivatives with respect to r and on the left-hand side of (28) are approximated by first-order accurate upwind differences and the distribution function at a new time level is determined according to a Runge-Kutta scheme.

The resulting advection scheme (28) can be used for arbitrary Knudsen numbers, including free-molecular regime, in which the discontinuities of the distribution functions play important role, and the continuum region, in which the second order of accuracy is essential to correctly model the flow in the boundary layer.

The description of the method is complete once we describe the procedure of computing the macroscopic parameters (10) in the right hand side. The conventional non-conservative expressions can be written as

$$\begin{aligned}
 n u_2 n T + n u_2 &= \int_{-1}^1 \int_{-1}^1 g_1 g_{1jk} \left(v_r + v_2 \right) g_1 + g_{2jk} A_{jk} \\
 (q_r, q_\varphi) &= \int_{-1}^1 \int_{-1}^1 g_1 g_{1jk} \left(v_r + v_2 \right) g_1 + g_{2jk} A_{jk}
 \end{aligned} \tag{29}$$

Here A_{jk} are the weights used in the quadrature formula. As a rule, the integrals with respect to φ are evaluated by using the composite Simpson rule, while the integrals with respect to μ are evaluated by applying the second-order accurate midpoint formula involving the distribution function values at the cell centers j, k .

Equations (17) for computing macroscopic parameters proposed in this paper take the following form (index i is omitted for simplicity):

$$\begin{aligned}
 \int_{-1}^1 \int_{-1}^1 H_1 \sin H_1^2 H_1 + H_{2jk} A_{jk} &= 0 \\
 \int_{-1}^1 \int_{-1}^1 (v_{rjk} (v_{2r} + v_2) H_1 + H_{2jk} A_{jk}) &= \frac{3}{4} (q_r, q_\varphi)
 \end{aligned} \tag{30}$$

System (30) for the macroscopic gas parameters n, u, T, q_r, q_φ is easily solved by Newton's method using (29) as the initial guess.

Therefore we have two methods of solving the formulated cylindrical Couette problem. The conventional method is given by the advection scheme (28) and non-conservative expressions (29). The method proposed in the present paper is a combination of the same implicit advection scheme (28) but uses (30) for computation of macroscopic quantities.

4.1.3 Convergence criteria

We use two different convergence criteria to stop the time marching to the steady state. For the method proposed in our paper we use the L_2 norm of the residual in conservation laws:

$$\text{Criteria}_{i=R/1} \text{ for all } i \in \mathbb{R} \quad \tau = \int_{-1}^1 \int_{-1}^1 H_1^2 H_1 + H_2 \quad i j k k A_{jk} \tag{31}$$

where ϵ is a small prescribed tolerance. Our choice is motivated by the fact that in the stationary limit the temporal derivative of the distribution function vanishes, and we must have $K_n = 0$. Then, expression (31) is a measure of how far the conservation laws are from the steady state.

For the conventional method it may not be possible to satisfy $Criteria_1$ due to the lack of the conservation property. Therefore we use the following criteria:

$$Criteria_2 = \frac{Q_{n+1,i} - Q_n}{t_2} \leq \epsilon \quad \text{for all } i \quad (32)$$

where $Q = (n, n, u, E)$, L_2 is the L_2 norm, ϵ is the small tolerance. We remark that in steady-state iteration methods [32, 2] the following condition is often used:

$$Criteria_3 = Q_{n+1} - Q_n \leq \epsilon \quad \text{for all } i \quad (33)$$

where n is now the number of iteration. However, in unsteady computations (32) is a more accurate criteria.

Remark. We note that since the advection scheme (28) is implicit the resulting method of the present paper is not conservative on unsteady solutions in the sense of [3]. However, it can be easily shown that in the steady-state limit we have the correct conservative approximation to the conservation laws.

4.1.4 Numerical tests

We have carried out a number of calculations for the rotation velocity $U = 0.5$, cylinder radii ratio $r_2 = 1.2$ and the range of Knudsen numbers $0.01 \leq Kn \leq 10$. The aim of the calculations was to compare the accuracy of the conventional non-conservative method (28),(29) and the its conservative modification (28),(30) proposed in this paper. We use the same tolerance value 10^{-5} both in (31) and (32). Since the advection scheme is essentially the same for both methods, the difference in the results can be attributed to the way the macroscopic parameters are computed, that is conservative (30) versus nonconservative (29).

Since our goal is to show the difference between two methods rather than to obtain a very accurate solution to the physical problem, we use in our convergence study a rather coarse non-uniform spatial mesh of $N_r = 50$ cells. In the molecular velocity space (v_x, v_y) , a sequence of uniform meshes was considered: 12 \times 50 cells, 20 \times 100 cells and 40 \times 200 cells.

We compare our results with those published in [29] obtained on an exceedingly fine mesh using a conventional steady-iteration method. In this reference the problem was solved for the BGK model ($Pr = 1$) and different values of the so-called rarefaction parameter :

$$\beta = 5Kn$$

We note that for this particular problem the S and BGK models yield the same results for the shear stress thus making it possible to do a direct comparison.

Table 1: Comparison with the results of [29] for the shear stress P_r . Molecular velocity mesh of 12x50 cells.

Kn	0	0.1	1	10	20
		9.0270	0.9027	0.09027	0.04514
[29]	0.06358	0.06357	0.05993	0.03412	0.02206
Conservative scheme	0.06392	0.06351	0.05973	0.03387	0.02198
Non-conservative scheme	0.06392	0.06350	0.05960	0.03227	0.01892

Table 2: The relative errors (in percents) of fulfilling the condition $r^2 P_r = \text{const}$ for the computation reported in Table 1.

Kn	0	0.1	1	10	20
		9.0270	0.9027	0.09027	0.04514
Conservative scheme	3.0756	2.9526	2.0248	0.9105	1.5610
Non-conservative scheme	3.0756	2.9277	1.7032	9.9976	31.2610

Table 1 shows the results for the shear stress P_r for different values of Kn and the fixed molecular velocity mesh of 12x50 cells in the (x, y) plane. Table 2 contains the relative errors (in percents) of fulfilling the condition $r^2 P_r = \text{const} = A$ which is the sequence of the kinetic equation. It is obvious that for $\text{Kn} = 1$ both conservative and non-conservative methods produce accurate results on the given rather coarse computational mesh. However, as the Knudsen number decreases the non-conservative method starts losing its accuracy even for these rather moderate values of Kn whereas the conservative scheme maintains its high accuracy. This is also evident from Table 2.

Table 3: The relative errors (in percents) of fulfilling the condition $r^2 P_r = \text{const}$.

Kn	1	0.1	0.03	0.01
Conservative scheme				
mesh of 12x50 cells	2.1079	0.8134	2.0863	5.2832
mesh of 20x100 cells	1.5387	0.3135	0.3773	1.3811
mesh of 40x200 cells	1.0896	0.4348	0.3303	0.6908
Non-conservative scheme				
mesh of 12x50 cells	1.8230	8.5605	94.9058	not available
mesh of 20x100 cells	1.5119	0.5854	6.9609	18.4220
mesh of 40x200 cells	1.0719	0.4023	0.2796	2.9190

Unfortunately, the data in [29] does not allow us to carry out the comparison for

smaller Kn numbers for which the difference between conservative and non-conservative methods becomes more evident. We have thus carried out a separate convergence study with respect to the molecular velocity mesh for the same fixed spatial mesh of 50 cells. Since no reference solution is available to us we use the integral relation $r^2 P = \text{const}$ as the measure of the computational error. Table 3 contains the corresponding relative errors. It is obvious, that for a given molecular velocity mesh the non-conservative method can compete with the conservative one only up to a certain Knudsen number. As Kn decreases, the errors present in the nonconservative computations grow rapidly and at a certain value of Kn the nonconservative method may fail to provide a solution.

The conservative method gives an accurate solution for the shear stress already at the mesh of 20 100 cells. On the other hand, for Kn = 0.01 the result of the nonconservative method on the next mesh of 40 200 cells is still inferior to the conservative one obtained on the four times coarser mesh of 20 100 cells. We also note that a finer mesh requires more time steps until the converged solution is reached. This translates in a large gain in computational efficiency as well as memory requirements of the method proposed in this paper over a conventional non-conservative scheme. We also remark that the conventional non-conservative method with (30) converges perfectly to the steady state according to a commonly used criteria (32). However, the resulting solution may be exceedingly inaccurate.

Fig. 1 shows distributions of density and temperature as functions of the normalized spatial coordinate $x = (r - r_1)/(r_2 - r_1)$ for Kn = 0.1 and two next molecular velocity meshes: 20 100 and 40 200 cells. Results of both conventional non-conservative and new conservative methods are shown. We observe, that for this Knudsen number the profiles obtained by the conservative method and that of the nonconservative method on the next mesh agree reasonably well. However, on the 20 100 mesh the nonconservative method is rather inaccurate for the temperature profile.

Fig. 2 shows distributions of density and temperature for Kn = 0.01 on all three meshes for the conservative method and on the next molecular velocity mesh for the nonconservative scheme. We remind the reader that on coarser meshes the latter method either fails to provide a solution or is very inaccurate. It is obvious, that density is computed accurately by the conservative method on all meshes; for temperature the result on the coarsest mesh is less accurate. Effectively, the results of the conservative scheme on two next meshes virtually coincide. On the other hand, the nonconservative method does not provide an acceptable solution even on the next mesh of 40 200 cells, especially for the temperature profile. This observation is in line with Table 3. We also note that when the molecular velocity mesh is further refined to 80 400 cells, the nonconservative solution for temperature does become closer to the conservative one computed on the mesh of 40 200 cells.

4.2 Transverse supersonic flow over a plate

We study transverse flow of a rarefied gas past a zero-thickness plate of finite width L . Both monatomic and diatomic flows are considered. A detailed setup of the problem can be found in [27, 34]. The free stream is characterized by the density n , velocity U , temperature T . We introduce a coordinate system with the x axis aligned with the normal to the plate, and y and z axes directed along the plate and spanwise. The plate is assumed to be homogeneous. Then the distribution function does not depend on z . The boundary condition of complete temperature accommodation of molecules to the surface temperature T_w is used throughout.

All calculations were performed for the non-dimensional freestream velocity $U = 3$ and plate temperature $T_w = 2$. For the monatomic gas we use $Pr = 23$ in the Shakhov model and $\gamma = 5/2$ (hard spheres). The diatomic gas is taken to be nitrogen with $B = 2$ which corresponds to the free-stream temperature 183 K. We study the influence of the Knudsen number and degrees of freedom (monatomic versus diatomic gas) on distribution of macroscopic parameters as well as the aerodynamic characteristics of the plate such as the drag C_D and heat transfer C_H coefficient given by the following expressions

$$C_D = \frac{2}{U^2} \int_0^L (P_{xx}(0,y) - P_{xx}(L,y)) dy$$

$$C_H = \frac{1}{L} \int_0^L (E_x(0,y) - E_x(L,y)) dy$$

Here the free-stream energy flux is $E_x = \frac{1}{2}(U^3 + \frac{5}{2}U)$ for the monatomic gas and $E_x = \frac{1}{2}(U^3 + \frac{7}{2}U)$ for the diatomic gas.

4.2.1 Method of the solution

The problem is solved in the non-dimensional variables as given by (4) so that the plate corresponds to $x = 0, 1 \leq y \leq 1$. Since the distribution function and macroscopic parameters do not depend on z the dimension of the problem can be reduced by eliminating the molecular velocity component z normal to the plane of the flow [8]. As a result, the distribution function depends on time t , two spatial coordinates x, y and two molecular velocity components v_x, v_y . The resulting kinetic equation is thus four-dimensional.

We incorporated the proposed conservative procedure into a implicit finite-volume TVD scheme for the kinetic equation, similar to (28). For $Kn = 0.3$ we use a non-uniform spatial mesh of 130 180 cells in the computational domain $55 \times 8, y = 10$. The cell size varied from 0.1 to 0.2 away from the plate to 0.002 in the Knudsen layer for the spatial mesh. For $Kn = 1$ a different mesh of 140 165 cells was used with the

domain size $15 \times 15, 15$. The computational domain in the molecular velocity space was $9, 0_y$

15. The computational domain in the molecular velocity space was $9, 0_y$. Here we used the symmetry of the velocity distribution function with respect to v_y . The mesh used was uniform with $\Delta = 0.45$. The fourth-order composite Simpson rule is used for constructing the weights A and evaluating integrals with respect to the molecular velocity.

Kn	C_D			C_H		
	0.003	0.03	0.3	0.003	0.03	0.3
= 090	1.644	1.585	1.759	0.025	0.0633	0.1897
= 045	1.641	1.673	1.845	0.024	0.0664	0.1966
= 025	1.641	1.673	1.845	0.024	0.0665	0.1966

Table 4: Dependence of C_D and heat transfer C_H coefficients on Δx (monatomic gas).

4.2.2 Influence of Δx

We study influence of the cell size in the molecular velocity mesh on the accuracy of the solution. To do so, we consider in addition to the basic molecular velocity mesh with $\Delta x = 0.05$ two more meshes: a coarse mesh with $\Delta x = 0.1$ and a fine mesh with $\Delta x = 0.025$. The results obtained with the finest mesh are used as the reference. It is well known, that one can expect to obtain a reasonable accuracy only if $\Delta x \leq \lambda/2$. However, due to the conservative nature of the method one may hope to get acceptable results with larger Δx , especially for small Knudsen numbers. In fact, this property of conservative methods is often used in computations with the exact Boltzmann equations [7] in order to reduce the cost of evaluating the 6-dimensional collision integral. We note however, that the numerical solution of the exact kinetic equation does not require the computation of the macroscopic parameters at each time step since they are not part of the equation. As a result, we cannot automatically generalize this property of conservative methods to model kinetic equations.

Table 4 shows aerodynamic coefficients of the plate as a function of Δx . It is obvious that for the smallest $Kn = 0.003$ the computed values of drag and heat transfer coefficients are very close for all meshes. When the Knudsen number increases so that the flow becomes more rarefied we begin to see the difference. For $Kn = 0.3$ the coarsest mesh leads to an error in the aerodynamics coefficients at about 35%, which may be considered as significant.

Figs. 3-4 present distribution of density and pressure over the both sides of the plate for $Kn = 0.3$ as a function of x . We see that on the upwind side the solutions corresponding to $\Delta x = 0.05$ and $\Delta x = 0.025$ are virtually identical whereas the solution with $\Delta x = 0.1$ has an error of about 6%. For the downwind side the influence of Δx is somewhat larger the solutions on two finest meshes being different of around 5% for density and 3% for pressure. The coarse mesh computation has a significantly larger error. Figs. 5-6 present the same convergence study but for a smaller Knudsen number $Kn = 0.003$. We see that solutions on two finest meshes ($\Delta x = 0.05$ and $\Delta x = 0.025$) are virtually identical. However, for the downwind side the use of $\Delta x = 0.1$ still gives a visible error. The observed errors in pressure profiles for results on different velocity meshes are consistent with those in the drag coefficients given in Table 4.

The numerical examples presented in this subsection show that overall it is sufficient to use $\Delta x = 0.05$, especially for small Knudsen numbers when the flow is in a near-continuum

	Kn	0.003	0.01	0.1	1	10	
monatomic	C_D	1.641	1.656	1.723	2.091	2.653	2.947
	C_H	0.024	0.039	0.116	0.330	0.558	0.652
nitrogen	C_D	1.704	1.705	1.782	2.161	2.708	2.947
	C_H	0.021	0.034	0.103	0.290	0.460	0.520

Table 5: Drag C_D and heat transfer C_H coefficients for $U = 3$ and $T_w = 2$.

regime. The use of smaller is justified only if an accurate computation of the low-density region behind the plate for transitional and large Knudsen numbers is necessary. This is due to the fact that for these Kn discontinuities of the velocity distribution function originating from the edges of the plate do not diminish rapidly enough in that region. In this situation one may use for better efficiency a non-uniform molecular velocity mesh refined towards the origin $x = y = 0$.

4.2.3 Comparison of monatomic and diatomic results

Table 5 contains dependencies of the drag C_D and heat transfer C_H coefficients for both gases. We first note that in the limiting case $Kn = \infty$ and given boundary conditions on the plate the drag coefficient is the same for both models. The heat transfer coefficient is different though. For finite Knudsen numbers we see clear influence of the number of degrees of freedom on the aerodynamic properties of the plate in the whole range of Knudsen numbers.

We also note that in order to cross check our method we have computed the drag and heat coefficients in Table 5 for $Kn = 1$ by the code from [34]. Identical results have been obtained.

Fig. 7,8 show the density and temperature profiles along the symmetry line (normal to the plate) for the transitional flow with $Kn = 0.1$. The position of the plate corresponds to the origin $x = 0$. We observe typical profiles, with a tendency to the formation of the bow shock wave and the sharp boundary layer upstream of the plate and a region of low density after the plate. The flow is overall far from equilibrium. It is especially well seen from the profiles of T_i and T_r for nitrogen, which are quite different around the plate. The temperature jump on the plate is quite large. However, in the far field x the flow begins to resemble continuum.

For the second much smaller Knudsen number $Kn = 0.003$ we see a standard flow pattern with a bow shock wave and exceedingly thin boundary layer with very sharp gradients of density and temperature. The temperature jump is negligible and the flow is in equilibrium everywhere except at the shock front and the Knudsen layer. Fig. 9 shows

flow streamlines for nitrogen. We clearly see the formation of the recirculation zone as the Knudsen number is decreased.

5 Conclusions

A conservative procedure for evaluating macroscopic parameters of the gas in the discrete ordinate method for the nonlinear model kinetic equations of Shakhov and Rykov has been presented. Conservation laws are satisfied for arbitrary values of the Knudsen number. Additionally, the correct evaluation of the heat flux is ensured in the limit of small Knudsen numbers.

The proposed method has been successfully used to calculate the cylindrical Couette flow and supersonic transverse flow past a flat plate in the broad range of the Knudsen number. The numerical results show that our method leads to significant savings in computer time and memory and is robust enough to be used in supersonic flows with sharp gradients.

Acknowledgments. The author acknowledges the financial support provided by the PRIN programme (2004-2006) of Italian Ministry of Education and Research (MIUR). The author would also like to thank E.M. Shakhov and V.A. Rykov for many valuable discussions on the model kinetic equations and discrete ordinate method as well as anonymous referees whose remarks helped improve the paper significantly.

References

- [1] K. Aoki, K. Kanba, and S. Takata. Numerical analysis of a supersonic rarefied gas flow past a flat plate. *Phys. Fluids*, 9(4):1144-1161, 1997.
- [2] K. Aoki, H. Yoshida, and T. Nakanishi. Inverted velocity profile in the cylindrical Couette flow of a rarefied gas. *Physical Review E*, 68(016302), 2003.
- [3] V.V. Aristov. Method of adaptive meshes in velocity space for the intense shock wave problem. *USSR J. Comp. Math. Math. Phys.*, 27:261-267, 1977.
- [4] V.V. Aristov and F.G. Cheremisin. A conservative splitting method for solving the Boltzmann equation. *USSR J. Comp. Math. Math. Phys.*, 20(1):191-207, 1980.
- [5] V.V. Aristov and S.A. Zabelok. A deterministic method for solving the Boltzmann equation with parallel computations. *Comp. Math. Math. Phys.*, 42(3):406-418, 2002.
- [6] P. L. Bhatnagar, E. P. Gross, and M. Krook. A model for collision processes in gases. I. Small amplitude processes in charged and neutral one-component systems. *Phys. Rev.*, 94(511):1144-1161, 1954.
- [7] F.G. Cheremisin. Conservative method for computing the Boltzmann collision integral. *Dokl. Akad. Nauk.*, 355(1):535-56, 1997.
- [8] C.K. Chu. Kinetic-theoretic description of the formation of a shock wave. *Phys. Fluids*, 8(1):122-2, 1965.

- [9] S.K. Godunov. A finite difference method for the computation of discontinuous solutions of the equations of fluid dynamics. *Mat. Sbornik*, 47:357-393, 1959.
- [10] M.I. Gradoboev and V.A. Rykov. Conservative method for numerical solution of the kinetic equations for small Knudsen numbers. *Comp. Math. Math. Phys.*, 34(2):246-266, 1994. check the title.
- [11] A.V. Gusarov and I. Smurov. Gas-dynamic boundary conditions of evaporation and condensation: numerical analysis of the Knudsen layer. *Phys. Fluids*, 14(12):4242-4255, 2002.
- [12] L.H. Holway. New statistical models for kinetic theory: methods of construction. *Phys. of Fluids*, 9(9):1658-1673, 1966.
- [13] M. Ya. Ivanov and R. Z. Nigmatullin. Implicit scheme of S.K. Godunov with increased order of accuracy for Euler equations. *USSR Comp. Math. Math. Phys.*, 27(11):1725-1735, 1987.
- [14] G.S. Jiang and C.W. Shu. Efficient implementation of weighted ENO schemes. *J. Comput. Phys.*, 126:202-212, 1996.
- [15] V. P. Kolgan. Application of the minimum-derivative principle in the construction of finite-difference schemes for numerical analysis of discontinuous solutions in gas dynamics. *Transactions of the Central Aerohydrodynamics Institute*, 3(6):6877, 1972. in Russian.
- [16] V. P. Kolgan. Finite-difference schemes for computation of three dimensional solutions of gas dynamics and calculation of a flow over a body under an angle of attack. *Transactions of the Central Aerohydrodynamics Institute*, 6(2):16, 1975. in Russian.
- [17] A.G. Kulikovskii, N. V. Pogorelov, and A. Yu. Semenov. *Mathematical Aspects of Numerical Solution of Hyperbolic Systems*. Chapman and Hall, 2002. Monographs and Surveys in Pure and Applied Mathematics, Vol. 118.
- [18] I. N. Larina and V. A. Rykov. Diatomic rarefied flow past a sphere on the basis of kinetic equations. *Dokl. Akad. Nauk. USSR*, 227(1):6062, 1976.
- [19] I. N. Larina and V. A. Rykov. Diatomic rarefied flow past a sphere. In *Numerical methods in rarefied gas dynamics. Volume 4*, pages 526-8. Dorodnicyn Computing Center of Soviet Academy of Sciences. *Soobsheniya po prikladnoy matematike.*, 1979.
- [20] I. N. Larina and V. A. Rykov. Hypersonic flows of a rarefied gas past conical bodies. In *Soobsheniya po prikladnoy matematike*. Dorodnicyn Computing Center of Soviet Academy of Sciences, 1990.
- [21] J.A. Lordi and R.E. Mates. Rotational relaxation in nonpolar diatomic gases. *Phys. Fluids*, 13(2):291-308, 1970.

- [22] L. Mieussens. Discrete-velocity models and numerical schemes for the Boltzmann-BGK equation in plane and axisymmetric geometries. *J. Comput. Phys*, 162(2):429-466, 2000.
- [23] A. Raines. Study of a shock wave structure in gas mixtures on the basis of the Boltzmann equation. *European Journal of Mechanics B/Fluids*, 202:599610, 2002.
- [24] V. A. Rykov. A model kinetic equation for a gas with rotational degrees of freedom. *Fluid Dynamics*, 10(6):959966, 1975.
- [25] E. M. Shakhov. Approximate kinetic equations in rareed gas theory. *Fluid Dynamics*, 3(1):156161, 1968.
- [26] E. M. Shakhov. Generalization of the Krook kinetic relaxation equation. *Fluid Dynamics*, 3(5):142145, 1968.
- [27] E. M. Shakhov. Transverse ow of a rareeld gas around a plate. *Fluid Dynamics*, 7(6):961 966, 1972.
- [28] E. M. Shakhov. *Method of investigation of rareed gas ows*. M.: Nauka, 1974. in Russian.
- [29] F. Sharipov and G. M. Kremer. Nonlinear Couette ow between two rotating cylindres. *Transport Theory and Statistical Physics*, 25(2):217229, 1996.
- [30] F. Sharipov and V. Seleznev. Data on internal rareed gas ows. *J. Phys. Chem. Ref. Data*, 27(3):657706, 1998.
- [31] C.-W. Shu. An overview on high order numerical methods for convection dominated PDEs. In T.Y. Hou and E. Tadmor, editors, *Hyperbolic Problems: Theory, Numerics, Applications*, pages 7988. Springer-Verlag, Berlin, 2003.
- [32] T. Soga and H. Oguchi. A nonlinear analysis of cylindrical Couette ow. In *Rareed Gas Dynamics. Proc. 9th Int. Symp.* DFVLR Press, Porz-Wahn, Germany, 1974. Paper No. A. 17.
- [33] V. A. Titarev. Towards fully conservative numerical methods for the nonlinear model Boltzmann equation. In *Preprint NI03031-NPA*, page 13. Isaac Newton Institute for Mathematical Sciences, University of Cambridge, Cambridge, UK, 2003.
- [34] V. A. Titarev and E. M. Shakhov. Flow computation in the bottom vacuum region behind a plate in a hypersonic rareed gas stream. *J. Comp. Math. Math. Phys.*, 41(9):13721384, 2001.
- [35] E. F. Toro. *Riemann solvers and numerical methods for uid dynamics*. Springer-Verlag, 1999. Second Edition.

- [36] B. van Leer. Towards the ultimate conservative difference scheme V: a second order sequel to Godunov's method. *J. Comput. Phys.*, 32:101-136, 1979.
- [37] J.Y. Yang and J.C. Huang. Rarefied flow computations using nonlinear model Boltzmann equations. *J. Comput. Phys.*, 120(2):323-339, 1995.
- [38] V.I. Zhuk, V.A. Rykov, and E.M. Shakhov. Kinetic models and the shock wave structure. *Fluid Dynamics*, 8(4):620-625, 1973.

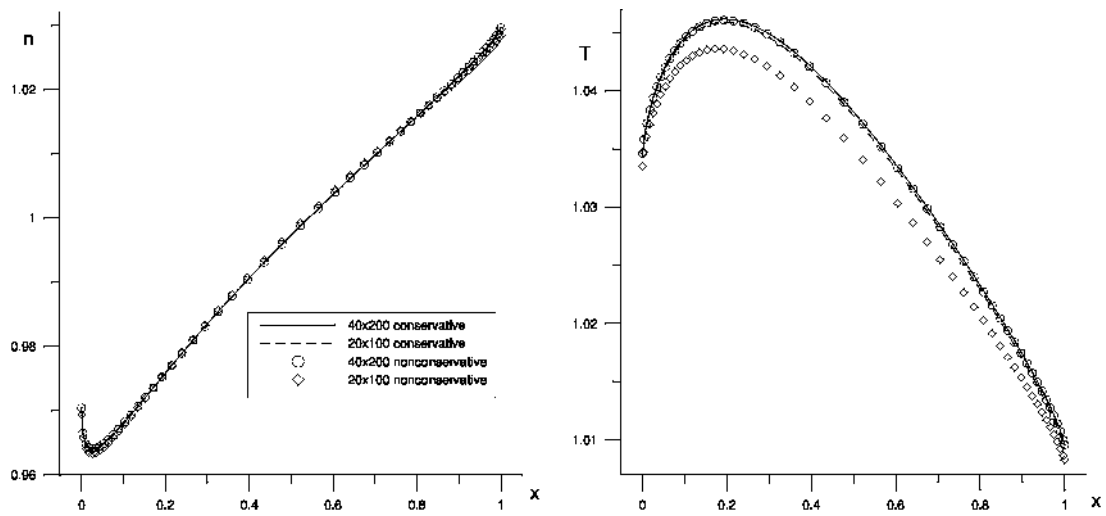


Figure 1: Density and temperature for the cylindrical Couette ow for $Kn = 01$.

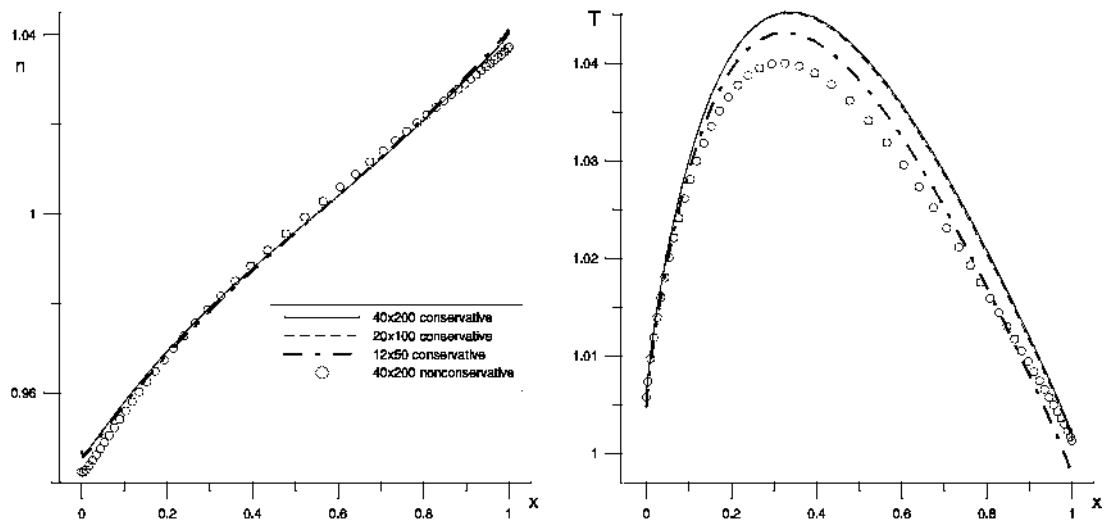


Figure 2: Density and temperature for the cylindrical Couette ow for $Kn = 001$.

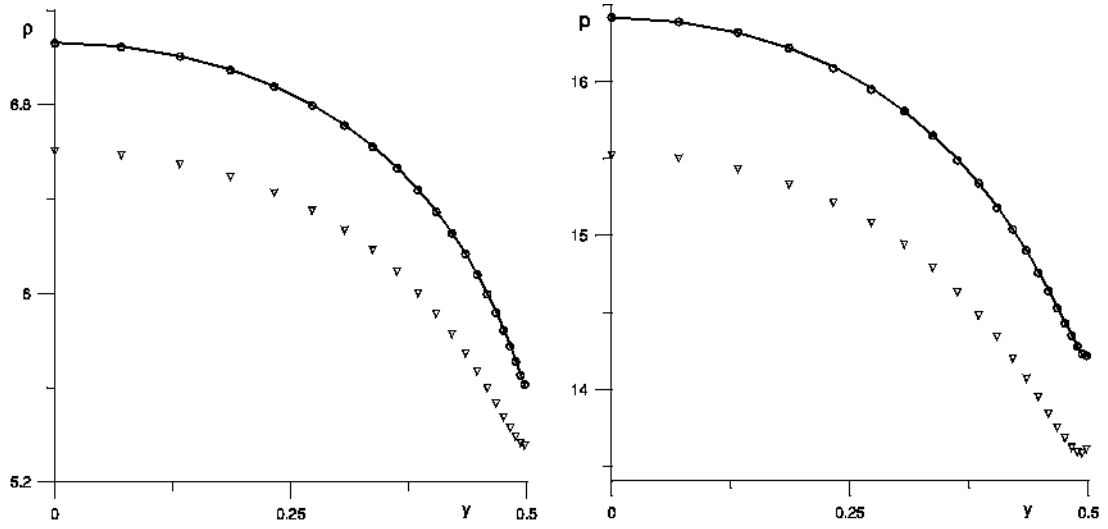


Figure 3: Density and pressure distribution over the upwind ($x = 0$) side of the plate for $Kn = 03$ and $Kn = 09$ (triangles), $Kn = 045$ (circles), $Kn = 025$ (solid line).

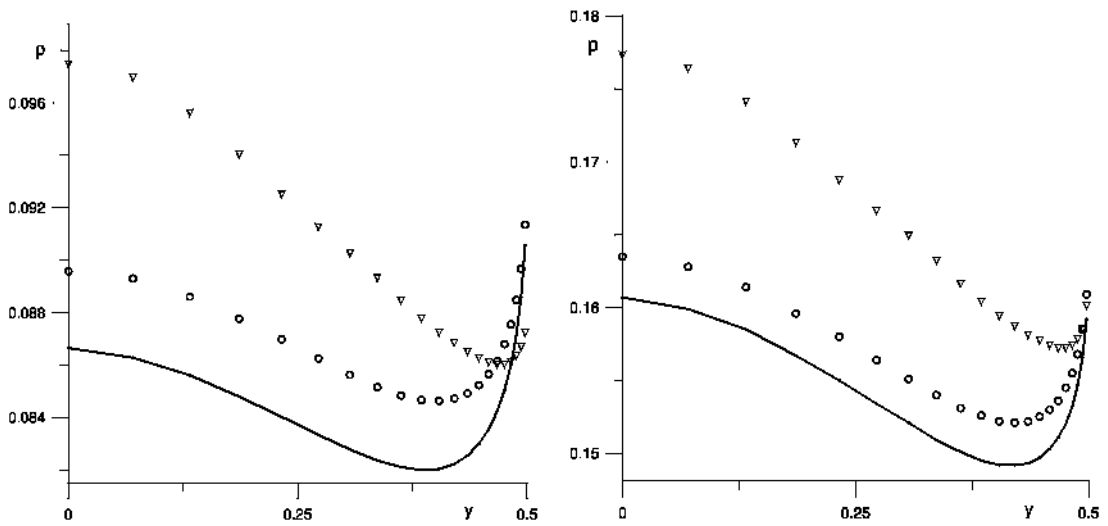


Figure 4: Density and pressure distribution over the downwind ($x = 0+$) side of the plate for $Kn = 03$ and $Kn = 09$ (triangles), $Kn = 045$ (circles), $Kn = 025$ (solid line).

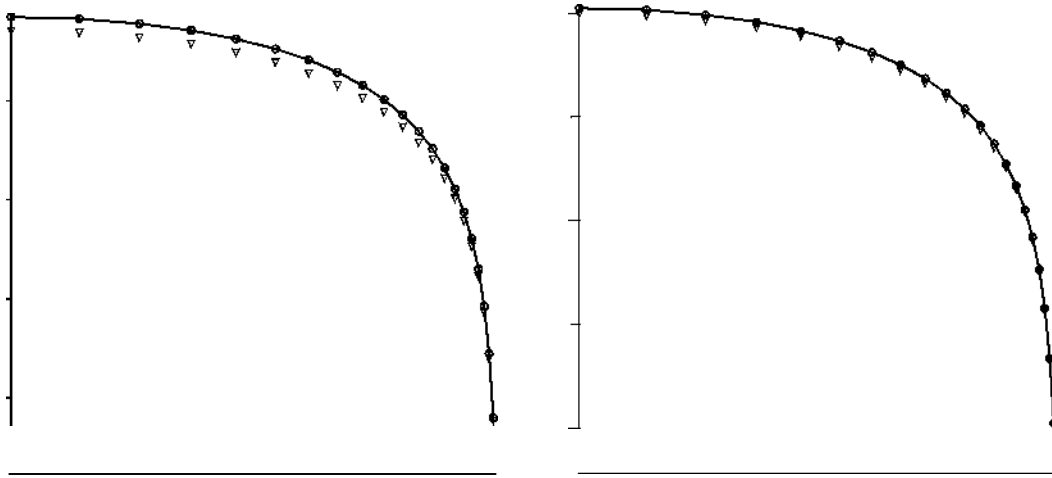


Figure 5: Density and pressure distribution over the upwind ($x = 0$) side of the plate for $Kn = 0003$ and $\beta = 025$ (solid line), 045 (circles), 09 (triangles).

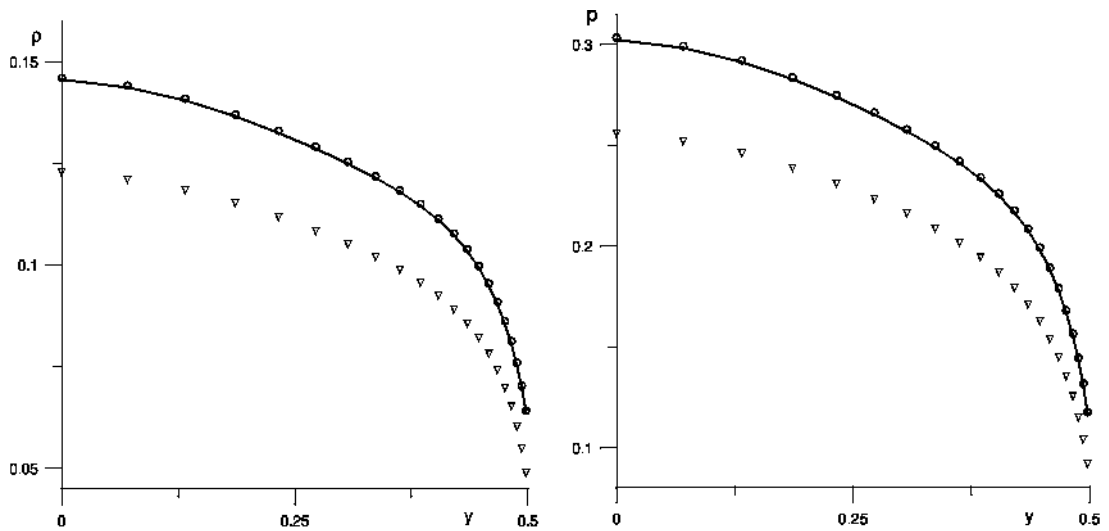


Figure 6: Density and pressure distribution over the downwind ($x = 0+$) side of the plate for $Kn = 0003$ and $\beta = 025$ (solid line), 045 (circles), 09 (triangles)

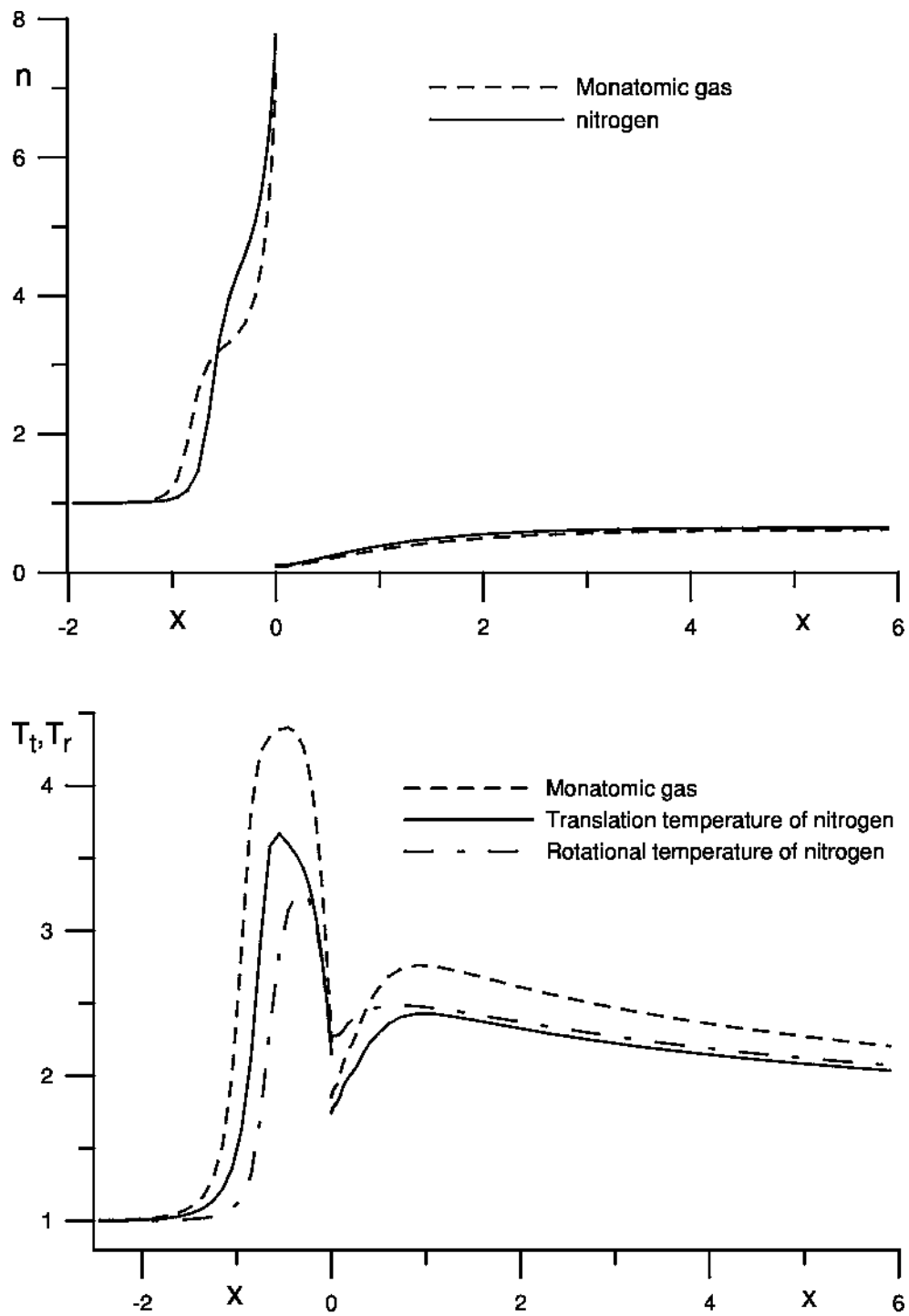


Figure 7: Density and temperature profiles along the symmetry line for $Kn = 0.1$

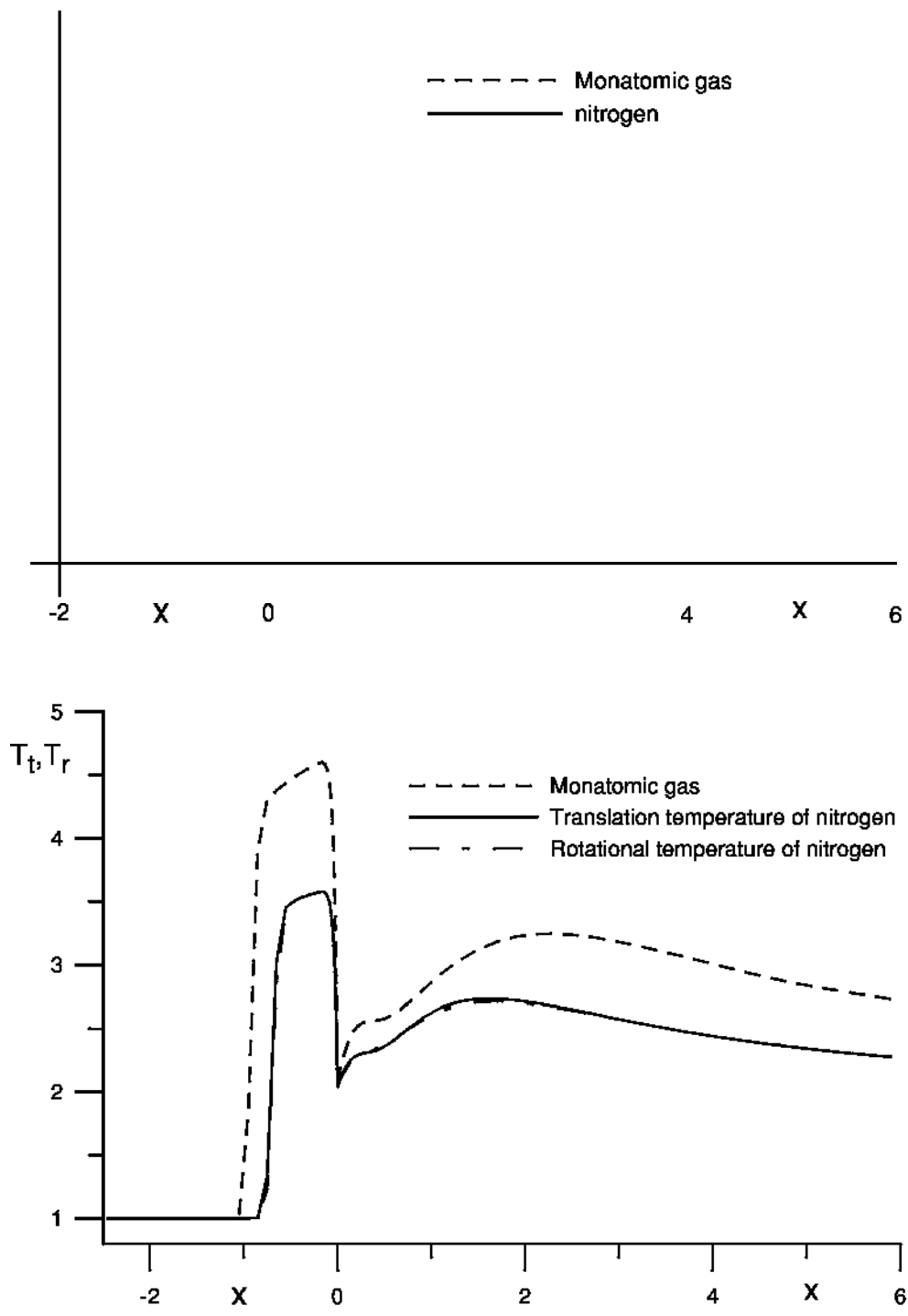


Figure 8: Density and temperature profiles along the symmetry line for $Kn = 0003$

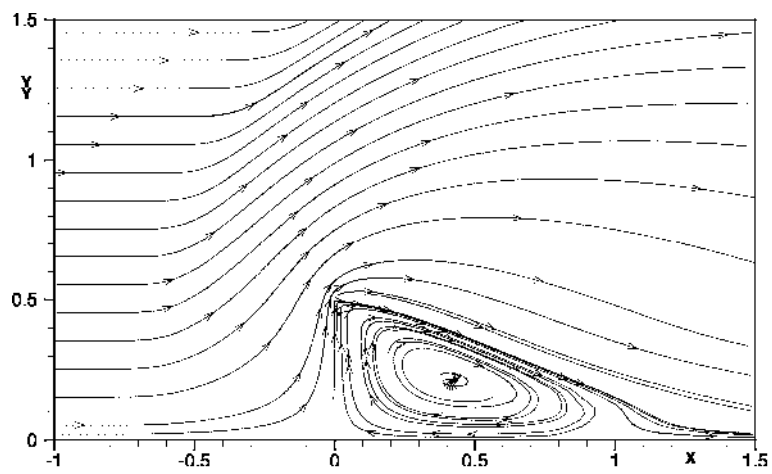
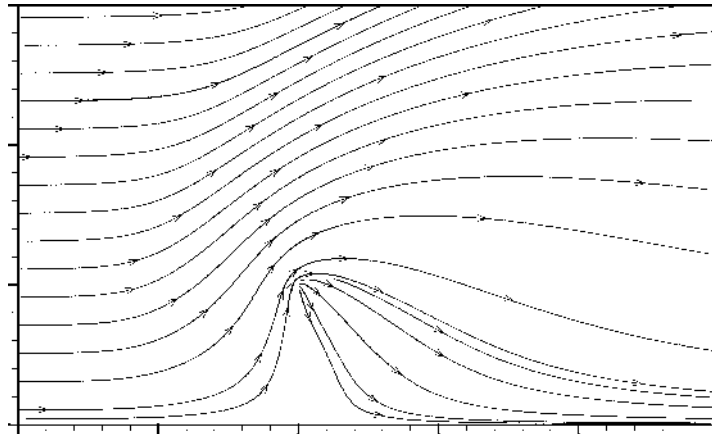


Figure 9: Flow streamlines in nitrogen: $Kn = 01$ (top) and $Kn = 0003$ (bottom).